A NOVEL MATLAB MODEL OF ANN BASED CONTROLLERS TO IMPROVE THE DYNAMIC PERFORMANCE OF A SHUNT ACTIVE POWER FILTER

D. GOWTAMI
st. Johns college of engineering & technology, yemmiganur, sai.gowtami10@gmail.com

S. RAVINDRA
st. Johns college of engineering & technology, yemmiganur, s.ravindra.sai@gmail.com

A. MALLIKARJUNA PRASAD
st. Johns college of engineering & technology, yemmiganur, mallikarjunaprasad0307@gmail.com

G. KISHORE
J.N.T.U.A, Anantapur, gudipatikishor@gmail.com

A NOVEL MATLAB MODEL OF
ANN BASED CONTROLLERS TO IMPROVE THE
DYNAMIC PERFORMANCE OF A SHUNT ACTIVE POWER FILTER

D.GOWTAMI, S.RAVINDRA,[1] A.MALLIKARJUNA PRASAD[2] & G KISHORE[3]

E-mail: chari.narasimhaiah@gmail.com

Abstract: This paper attempts to enhance the dynamic performance of a shunt-type active power filter. The predictive and adaptive properties of artificial neural networks (ANNs) are used for fast estimation of the compensating current. The dynamics of the dc-link voltage is utilized in a predictive controller to generate the first estimate followed by convergence of the algorithm by an adaptive ANN (*adaline*) based network. Weights in *adaline* are tuned to minimize the total harmonic distortion of the source current. Extensive simulations and experimentations confirm the validity of the proposed scheme for all kinds of load (balanced and unbalanced) for a three-phase three-wire system.

Keyword: -Adaline, current control, nonlinear load, shunt active power filter (APF), total harmonic distortion (THD), voltage source inverter.

1. INTRODUCTION

Harmonic compensations have become increasingly important in power systems due to the widespread use of adjustable-speed drives, arc furnace, switched-mode power supply, uninterruptible power supply, etc. Harmonics not only increase the losses but also produce unwanted disturbance to the communication network, more voltage and/or current stress, etc. Different mitigation solutions, e.g., passive filter, active power line conditioner, and also hybrid filter, have been proposed and used [1]–[8]. Recent technological advancement of switching devices and availability of cheaper controlling devices, e.g. ,DSP-/field-programmable-gate-array-based system, make active power line conditioner a natural choice to compensate for harmonics. Shunt-type active power filter (APF) is used to eliminate the current harmonics.

The dynamic performance of an APF is mainly dependent on how quickly and how accurately the harmonic components are extracted from the load current. Many harmonic extraction techniques are available, and their responses have been explored. Proposed techniques include traditional $d-q$ [2] and $p-q$ theory [3]–[5] based approaches and application of adaptivefilters [6], wavelet [7], genetic algorithm (GA), artificialneural network (ANN), etc., for quick estimation of the compensating current [8]. A critical evaluation of such techniques is recently reported by the authors [8].

Recently, ANNs have attracted much attention in different applications, including the APF [9]–[20], [22]. Dash *et al.* [14] computed the Fourier coefficients of the signal by using *adaline*, and Chen and O'Connell [15] used an ANN that is trained with GA and back propagation. Lai *et al.* [16] used a

Hopfield neural network for real-time computation of frequency and harmonic content of the signal. Improved performance has been observed compared to discrete Fourier transform, fast Fourier transform, or Kalman-filtering-based approaches.

Tey *et al.* [17] reported a modified version of [10]. An additional PI controller is used to regulate the dc-link voltage. A full "neuromimetic" strategy involving several *adalines* has been reported by Abdeslam *et al.* [18]. The controller can adapt for unbalance and change in working conditions. Lin [19] proposed an intelligent neural-network-based harmonic detection, which is first trained with enough data (1400 patterns). The working model could compute the harmonic components with only onehalf of the distorted wave. An *adaline*-based harmonic compensation is reported by Singh *et al.* [20]. Weights are computed online by the LMS algorithm. Luo *et al.* [21] demonstrated a 200-kVA laboratory prototype for a combined system for harmonic suppression and reactive power compensation using an optimal nonlinear PI controller, whereas a two-stage recursive least square based *adaline* is reported by Chang *et al.* [22] for harmonic measurement.

Note that parallel developments on predictive control techniques are reported for power controllers. These are also applied to APF [23], [24]. The implementation of APF using power balance at the dc link is reported by Singh *et al.* [25]. The dc-link voltage has been used to find the peak magnitude of the supply current for self-supporting dc bus. However, no detail analysis of the dynamics of the dc-link voltage is available. This paper is an integration of predictive and adaptive control techniques for fast convergence and reduced computations. Two ANN-based controllers are used

for such purpose. The predictive controller generates the first estimate of the compensating current quickly after the change in load is detected. The change in voltage across the capacitor is used for this purpose. This is followed by an *adaline*-based controller to fast converge to the steady value. This paper is organized in Eight sections. Section II deals with the Basic Block Diagram. Section III Estimation of Current Reference. Regulation of DC link Voltage in APF is covered in Section IV. Fastestimationof compensatingcurrent using ANN is presented in Section V. Section VI presents the Adaptive Current Detection Technique, Section VII presents the MATLAB Model and Simulation results. Section VIII concludes the work.

2. BASIC BLOCK DIAGRAM

A general block diagram of a APF with a non-linear load is shown below. Two ANN-based controllers are used for such purpose. The predictive controller generates the first estimate of the compensating current quickly after the change in load is detected. The change in voltage across the capacitor is used for this purpose. This is followed by an *adaline*-based controller to fast converge to the steady value.

3. ESTIMATION OF CURRENT REFERENCE

Fig. 1(a) shows the APF compensating a nonlinear load. Fig. 1(b) shows the corresponding schematic diagram. A general expression for the load current [corresponding to Fig. 1(b)] is $iL(t) = i\alpha1(t) + i\beta1(t) + ih(t)$.(1)
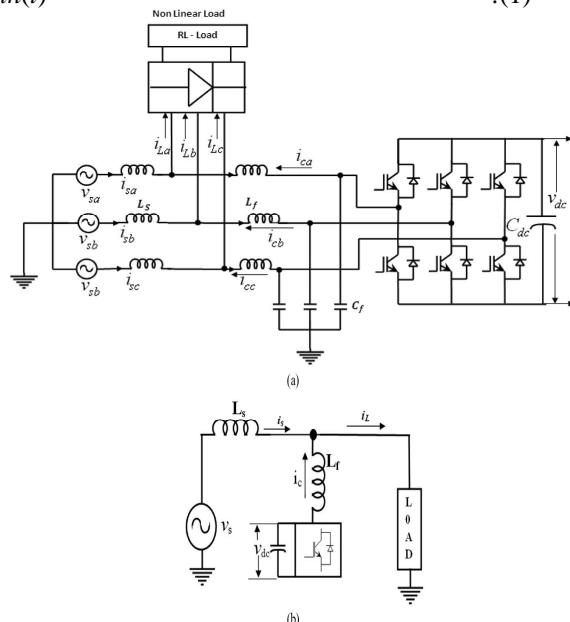
Fig. 1. (a) APF to compensate for a nonlinear load. (b) Single phase of shunt APF.

The in-phase and quadrature components of the phase current atfundamental frequency are $i\alpha1$ and $i\beta1$, respectively. All otherharmonics are included in ih. The per-phase source voltage andthe corresponding

in-phase component of the load current maybe expressed as

$$vs(t) = Vm \cos \omega t \quad (2)$$
$$i\alpha1(t) = I\alpha1 \cos \omega t \quad .(3)$$

Assuming that the APF will compensate for harmonic and reactive power, the compensating current becomes $ic(t) = iL(t) - i\alpha1(t) = iL(t) - I\alpha1 \cos \omega t$ (4)

where $I\alpha1$ is the peak magnitude of the in-phase current that themains should supply and hence needs to be estimated. Once $I\alpha1$estimation is over, the reference current for the APF may easilybe set as per (4). $iL(t)$ may be measured using current sensors.In our proposed scheme, estimation of $I\alpha1$ is carried out by twostages. A single-layer ANN-based algorithm first predicts the value of $I\alpha1$ following which an *adaline*-based ANN is usedfor fast convergence. Note that the inverter also draws a smallcurrent ($is\alpha(t)$) to maintain the dc-link voltage.

4. REGULATION OF DC-LINK VOLTAGE IN APF

The dynamics of the dc-link voltage is an indirect measure of the performance of the APF. Whenever there is a change in the load, the voltage across the dc-link capacitor also undergoes a corresponding change. A controller is used to keep the voltage regulated at a desired value. In this section, asimple analysis of the dynamics of the dc-link voltage is first carried out. Parameters that govern the dynamics are identified, following which an algorithm is developed to estimate the compensating current of the APF.

To maintain the dc-bus voltage to a desired magnitude, the capacitor draws in-phase (i.e., in phase with the source voltage) current $is\alpha$. This is in addition to the compensating current ic. From the power balance equation

$$p_{dc} = C_{dc} v_{dc} \frac{dv_{dc}}{dt} \quad (5)$$

where p_{dc} is the power required to maintain the voltage v_{dc} across the dc link.

From the power balance equation

$$\sum_{i=a,b,c} v_{si}(t)i_{s\alpha i}(t) - \sum_{i=a,b,c} R_f(i_{s\alpha i}^2(t) + i_{ci}^2(t))$$
$$- \frac{1}{2}\sum_{i=a,b,c} L_f \frac{d}{dt}(i_{s\alpha i}^2(t) + i_{ci}^2(t)) =$$
$$i_{dc}(t)v_{dc}(t) =$$
$$p_{dc} \quad (6)$$

where Rf and Lf are the resistance and inductance of the inductor that is connected in between the point of common coupling and the voltage source inverter. Note that $is\alpha$ suppliesthe system loss at the steady state and charges/dischargesthe capacitor during transient to maintain the dc-link voltage.

Considering that "power" is a scalar quantity, (6) for a balanced three-phase system may be expressed as

$$3v_s(t)i_{s\alpha}(t) - 3R_f(i_{s\alpha}^2(t) + i_c^2(t)) -$$

$$\frac{3}{2}L_f\frac{d}{dt}(i_{s\alpha}^2(t) + i_c^2(t)) = i_{dc}(t)v_{dc}(t) = p_{dc} \qquad (7)$$

Applying small perturbations in i_c, $i_{s\alpha}$, v_{dc}, and v_s, around an operating point, the following new set of variables may be obtained:

$$i_c(t)=I_c+\Delta i_c \qquad (8)$$

$$i_{s\alpha}(t) = I_{s\alpha}+\Delta i_{s\alpha} \qquad (9)$$

$$v_{dc}(t)=V_{dc}+\Delta V_{dc} \qquad (10)$$

$$v_s(t)=V_s+\Delta V_s \qquad (11)$$

where Ic, $Is\alpha$, and Vs are rms and Vdc is the dc value of the corresponding quantities at the operating point.

Again, in steady state

$$3V_sI_{s\alpha}-3R_f(I_{s\alpha}^2+I_c^2)=0 \qquad (12)$$

Substituting (8)–(12) in (7), the following equation is obtained:

$$3(\Delta v_sI_{s\alpha}+V_s\Delta i_{s\alpha})-6R_f(I_{s\alpha}\Delta i_{s\alpha}+I_c\Delta i_c)$$

$$3L_f(I_{s\alpha}\frac{d\Delta i_{s\alpha}}{dt}+I_c\frac{d\Delta i_c}{dt})=C_{dc}V_{dc}\frac{d\Delta v_{dc}}{dt} \qquad (13)$$

Converting the variables to s-domain and after rearranging, (13) may be expressed as

$$\Delta V_{dc}(s)=\frac{KG_s(s)G_1(s)G_2(s)}{1+KG_s(s)G_1(s)G_2(s)}\Delta V_{dc}^*(s)-$$

$$\frac{G_2(s)G_3(s)}{1+KG_s(s)G_1(s)G_2(s)}\Delta I_c(s)+\frac{G_2(s)G_4(s)}{1+KG_s(s)G_2(s)G_4(s)}\Delta V_s(s) \qquad (14)$$

where K is the small-signal gain.

Equation (14) confirms that the ripple in the dc-link voltage depends on $\Delta V*dc$, ΔIc, and ΔVs. In our present problem, the distortion in source voltage and reference dc-bus voltage is not considered. Therefore, (14) further modifies to

$$\Delta V_{dc}(s)= -\frac{G_2(s)G_3(s)}{1+KG_s(s)G_1(s)G_2(s)}\Delta I_c(s) \qquad (15)$$

This explores the possibility of extracting an estimate of the compensating current from the change in vdc.

The gains of the PI controller used to regulate the dc link voltage are governed by the following two inequalities [26]:
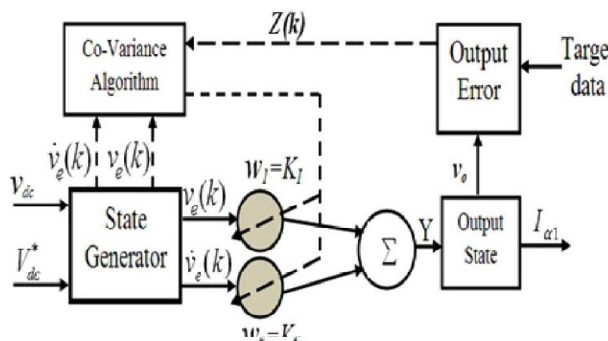

Fig 2. Block Diagram of ANN-Based Peak Value Predictor

$$I_s<\frac{C_{dc}V_{dc}^*}{3K_PL_f} \qquad (16)$$

$$I_s\leq\frac{K_PV_s}{2R_fK_P+L_fK_i} \qquad (17)$$

All the ac quantities in (16) and (17) are expressed as rms value. Is, $V*dc$, and Vs are the source current, reference dc-link voltage, and source voltage,

respectively. Equations (16) and (17) are used to generate an initial guess of KP and KI and also to set their limits.

5. FAST ESTIMATION OF COMPENSATING CURRENT USING ANN

An ANN-based PI controller plays a dual role. It ensures faster reference generation and is also accountable for better regulation of dc-bus voltage. The structure of the system (i.e., ANN-tuned adaptive PI controller) is shown in Fig. 2. To reduce computational burden, a single-layer ANN structure is used. The input vector as expressed in (18) is fed to the state exchanger. In our scheme, error voltage and its gradient are chosen as the state of the system to ensure faster corrective action

$$u=[V_{dc}^* v_{dc}]^T \qquad (18)$$

$$x_1=v_e(k) \qquad x_2=\frac{\delta x_1}{\delta k} \qquad (19)$$

where $ve(k) = V*dc - vdc(k)$. The output error $z(k)$ is represented as

$$z(k)=v_o(k)-v_o(k-1) \qquad (20)$$

The output $vo(k)$ is fed to output state to estimate $I\alpha1$.

Neuron cell generates controlling signal through interrelated gathering [27], [28] as

$$u(k) = u(k-1)\sum_{i=1}^{2}w_i(k)x_i(k) \qquad (21)$$

where wi is the weight of the system

Here, a neuron is trained by Hebb's rule [27], [28]. Therefore, the change of weight of the neuron cell at kth instant may be represented as

$$w_i(k+1)=(1-c)w_i(k)+\eta r_i(k) \qquad (22)$$

$$r_i(k)=z(k)u(k)x_i(k) \qquad (23)$$

where ri is the progressive signal, η is Hebb's studying ratio (learning rate), and "c" is a constant. Substituting (22) and (23) in (21), the following equation may be obtained:

$$\Delta w_i(k)= w_i(k+1)-w_i(k)$$

$$= -c[w_i(k)- \eta z(k)u(k)x_i(k)/c] \qquad (24)$$

$\Delta wi(k)$ is the change of weight at kth step. Weights of the neuron are tuned according to Hebb's assumption. Hebb's assumption is popularly known as the covariance algorithm.

$$\Delta w_i(k)=F_i(y_1(k),x_i(k)) \qquad (25)$$

where $Fi(*)$ is a function of both postsynaptic and presynaptic signals and $y1$ is the output of the individual neuron. If $Fi(*)$ is differentiable, then $\delta Fi/\delta wi$ may be represented as

$$-\!\!\!- = w_i(k)- -z(k)u(k)x_i(k) \qquad (26)$$

From (26), the change of weight in kth sample may be expressed as

$$\Delta w_i(k)= -c\frac{\delta F_i(k)}{\delta w_i(k)} \qquad (27)$$

Thus, by adjusting the values of $wi(k)$, KP and KI are tuned.

The weights $wi(k)$ are searched according to the negative slope of function $Fi(*)$. Equations (26) and (27) are used to tune the parameter used in (28) and

(29). Finally, for the PI controller, the weights are represented by

$$w_1(k+1)=w_1(k)+ \eta_I z(k)x_1(k) \quad (28)$$
$$w_2(k+1)=w_2(k)+ \eta_P z(k)x_2(k) \quad (29)$$

Whenever the ANN is initiated, it starts with a set of controller gains to generate the first estimate of the compensating current. These initial values of controller parameters are set by offline training of the ANN. The controller parameters are then adjustedfollowing (28) and (29) to regulate the dc-link voltage.

6. ADAPTIVE CURRENT DETECTION TECHNIQUE

The ANN in Section IV provides an initial guess for any change in system dynamics. To generate more accurate reference for APF, load current samples are fed to the *adaline*-based network shown in Fig. 3. *Adaline* is designed to minimize the total harmonic distortion (THD) of source current. Uncompensated source current sample $s(k)$ may be represented as

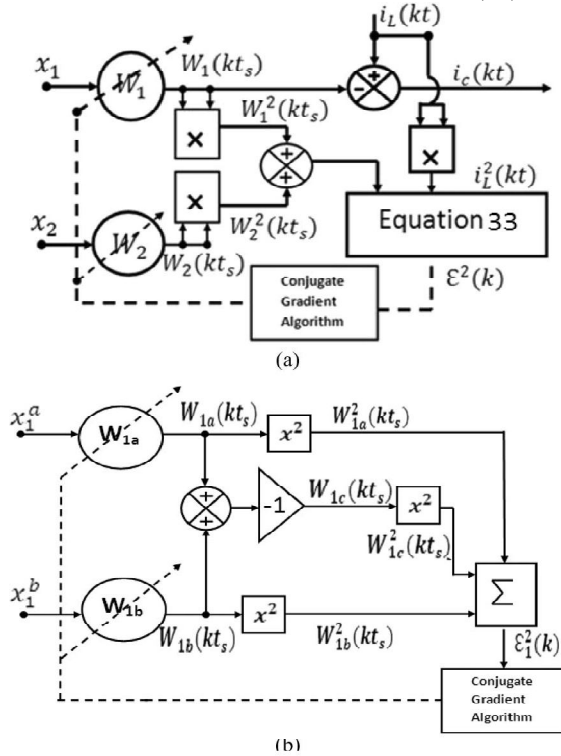$$s(k)=I_{\alpha1}\cos(\omega kt_s)+I_{\beta1}\sin(\omega kt_s)+ \quad (30)$$

(a)

(b)

Fig 3: a) Adaline Based Harmonic Extraction for a Three Phase Balanced Network b)Adaline Based Harmonic Extraction for a Three Phase UnBalanced Network

Where *ts* is the step size in discrete domain. The square of errorterms for *k*th sample may be expressed as

$$\varepsilon^2(k)=\left[\frac{\{s^2(k)-2s(k)a(k)\}}{a^2(k)}+1\right](31)$$

Where
$$a^2(k)= I^2_{\alpha1}(k)\cos^2(\omega kt_s)+I^2_{\beta1}(k)\sin^2(\omega kt_s) \quad (32)$$

Equation (31) may also be represented as

$$\varepsilon^2(k)=\left[\frac{\{s^2(k)-2s(k)[X^T(k)\bar{a}(k)\bar{a}^T(k)X(k)]\}}{X^T(k)\bar{a}(k)\bar{a}^T(k)X(k)}+1\right] \quad 33)$$

where the vector
$$\bar{a}(k) = [I_{\alpha1}(k),I_{\beta1}(k)] \quad (34)$$
and the input vector
$$X(k)=[\cos\omega kt_s,\sin\omega kt_s]^T \quad 35)$$

Equation (33) is further modified to fit in terms of a quadratic equation as

$$A\left\{\left[\bar{a}^T(k)X(k)\right]^T\left[\bar{a}^T(k)X(k)\right]\right\}- B\left[\bar{a}^T(k)X(k)\right]+C = 0 \quad (36)$$

Equation (36) is minimized by *conjugate gradient* (CG) method [27]–[29].

Thus, the error function (i.e., THD) is minimized to calculatethe in-phase component of the fundamental load current. The compensating current is then calculated according to (4). Convergence of this method is faster than existing *adaline*-based schemes due to the use of less number of tuning blocks. The orthogonal relationship between the input vectors reduces the computational burden of the system.

Fig. 3(a) shows the details of current detection for a threephase balanced system, while Fig. 3(b) shows the same for an unbalanced (three-phase and three-wire) network. $W1a$, $W1b$, and $W1c$ are the corresponding in-phase components of the current for phase-a, phase-b and phase-c, respectively.

7. MATLAB MODELLING

7.1 Block Diagram

A general block diagram of the PVA model for GUI environment of Simulink is given in Fig.4.Simulations have been conducted for balanced and unbalancedloads using SIMULINK for different controller configurations. The whole system is built in SIMULINK where the ANNroutine is called whenever necessary.

First, simulation study is made for the case with only predictivealgorithm. A quickestimate helped, the waveform quality is poor due to the lackof any corrective mechanism in the system. The simulation results obtained.Next, the adaptive algorithm is tried. Simulation have done to check the performance of thesystem for a step change in load. Balance three-phase nonlinearload is considered similar to the case with predictivealgorithm.

Now, to have the advantage of predictive and adaptive controllers, the system is run with both the algorithms. Fig4 show the situation with both the predictive and adaptive controllers in operation. The results have confirmed very satisfactory performance in terms of waveform quality and response time.

The controller is found to operate satisfactorily.The source current, load current, and compensating currentare shown in top-to-bottom order. The controller took 51 s toconverge, whereas the proposed controller with predictive andadaptive algorithm converged within less than one-quarter of acycle with acceptable current quality.
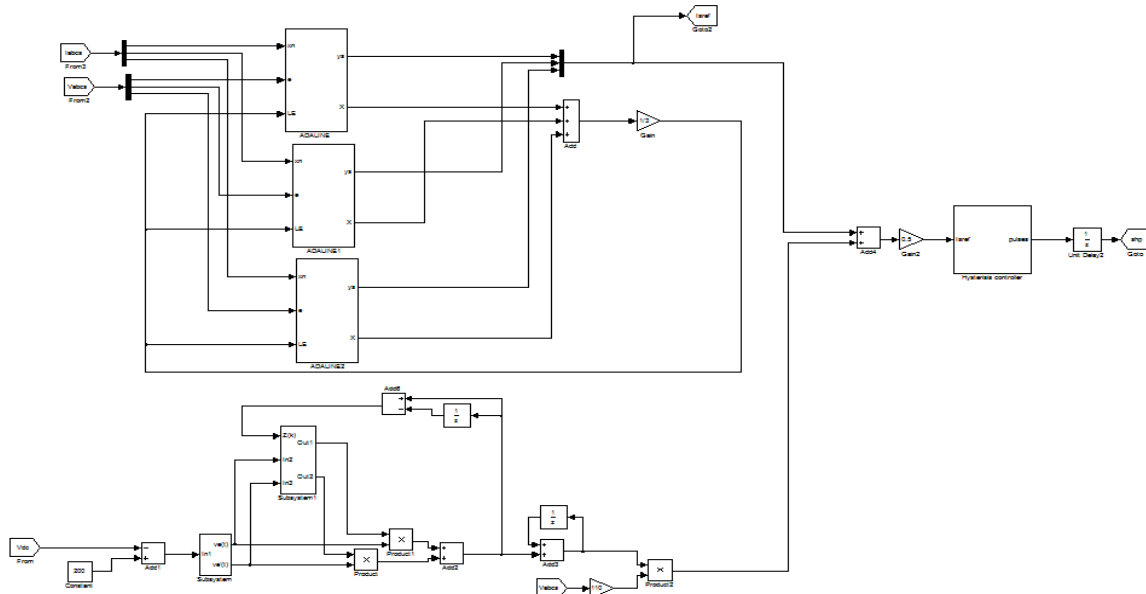

Fig 4: Operational functional block diagram of the ANN Model

8. RESULTS AND DISCUSSION

Simulations have been conducted for balanced and unbalanced loads.First simulation study is made for the case of only predictive algorithm Fig 5 gives simulation results with predictive ANN. Fig 6 gives simulation results of APF with adaline.Fig 7. Performanceof the APF with predictive and adaptive controllers.
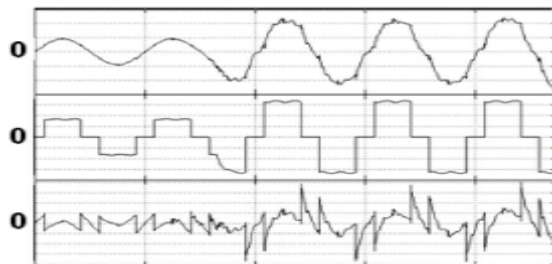

Fig. 5. Performance of the APF with predictive ANN (simulation results). Topwaveform: Source current of phase A (scale: 5 A/div). Middle waveform: Loadcurrent of phase A (scale: 5 A/div). Bottom waveform: Compensating currentof phase A (scale: 5 A/div). Time scale: 20 ms/div.
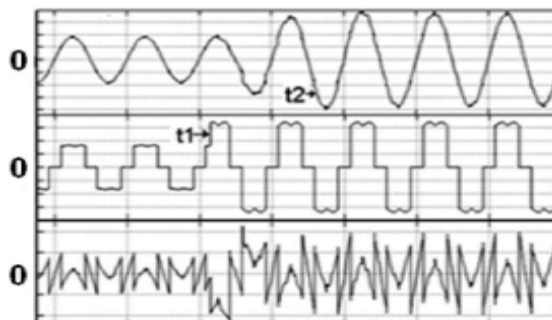

Fig. 6. Performance of the APF with *adaline* (simulation results). Top waveform: Source current of phase A (scale: 5 A/div). Middle waveform: Load current of phase A (scale: 5 A/div). Bottom waveform: Compensating current of phase A (scale: 5 A/div). Time Scale: 20 ms/div.Fig8: Current-Voltage (I-V) Characteristics of PVA.
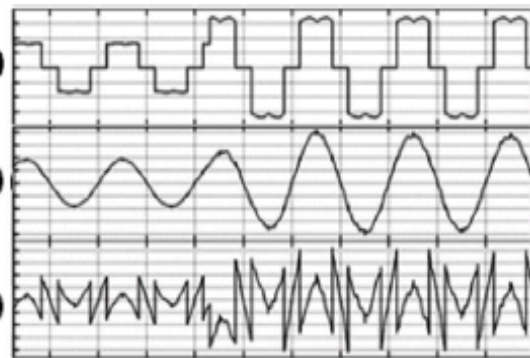

Fig. 7. Performance of the APF with predictive and adaptive controllers (simulation results). (a) Load current of phase A (scale: 5 A/div). (b) Source current of phase A (scale: 20 A/div). (c) Compensating current of phase A (scale: 5 A/div). Time scale: 10 ms/div.

9. CONCLUSION

An integration of predictive and adaptive ANN-based controllerfor a shunt-type APF has been presented in this paperto improve the convergence and reduce the computational requirement.The predictive algorithm is derived from an ANNbased PI controller used to regulate the dc-link voltage in theAPF. This is followed by an *adaline*-based THD minimization technique. *Adaline* is trained by CG method to minimize THD.Use of only two weights and two

input vectors makes the convergence very fast. The system is extensively simulated in MATLAB/SIMULINK.

REFERENCES

[1] B. Singh, K. Al-Haddad, and A. Chandra, "A review of active power filters for power quality improvements," *IEEE Trans. Ind. Electron.*, vol. 46, no. 5, pp. 960–971, Oct. 1999.

[2] S. Bhattacharya, T. M. Frank, D. M. Divan, and B. Banerjee, "Active filter system implementation," *IEEE Ind. Appl. Mag.*, vol. 4, no. 5, pp. 47–63, Sep./Oct. 1998.

[3] H. Akagi, Y. Kanazawa, and A. Nabae, "Instantaneous reactive power compensators comprising switching devices without energy storage components," *IEEE Trans. Ind. Appl.*, vol. IA-20, no. 3, pp. 625–630, May 1984.

[4] F. Z. Peng, G.W. Ott, Jr., and D. J. Adams, "Harmonic and reactive power compensation based on the generalized instantaneous reactive power theory for three phase four wire system," *IEEE Trans. Power Electron.*, vol. 13, no. 6, pp. 1174–1181, Nov. 1998.

[5] R. S. Herrera and P. Salmeron, "Instantaneous reactive power theory: A reference in the nonlinear loads compensation," *IEEE Trans. Ind. Electron.*, vol. 56, no. 6, pp. 2015–2022, Jun. 2009.

[6] H. Karimi, M. Karimi-Ghartemani, and M. R. Iravani, "An adaptive filter for synchronous extraction of harmonics and distortions," *IEEE Trans. Power Del.*, vol. 18, no. 4, pp. 1350–1356, Oct. 2003.

[7] M. Forghani and S. Afsharnia, "Online wavelet transform-based control strategy for UPQC control system," *IEEE Trans. Power Del.*, vol. 22, no. 1, pp. 481–491, Jan. 2007.

[8] A. Bhattacharya, C. Chakraborty, and S. Bhattacharya, "Current compensation in shunt type active power filters," *IEEE Ind. Electron. Mag.*, vol. 3, no. 3, pp. 38–49, Sep. 2009.

[9] A. Hamadi, S. Rahmani, and K. Al-Haddad, "A hybrid passive filter configuration for VAR control and harmonic compensation," *IEEE Trans. Ind. Electron.*, vol. 57, no. 7, pp. 2419–2434, Jul. 2010.

[10] B. Widrow and M. A. Lehr, "30 years of adaptive neural networks: Perceptron, madaline and backpropagation," *Proc. IEEE*, vol. 78, no. 9, pp. 1415–1442, Sep. 1990.

[11] C.-C. Tsai, H.-C. Huang, and S.-C. Lin, "Adaptive neural network control of a self-balancing two-wheeled scooter," *IEEE Trans. Ind. Electron.*, vol. 57, no. 4, pp. 1420–1428, Apr. 2010.

[12] A. Dinu, M. N. Cirstea, and S. E. Cirstea, "Direct neural-network hardware-implementation algorithm," *IEEE Trans. Ind. Electron.*, vol. 57, no. 5, pp. 1845–1848, May 2010.

[13] G. W. Chang, C.-I Chen, and Y.-F. Teng, "Radial-basis-function-based neural network for harmonic detection," *IEEE Trans. Ind. Electron.*, vol. 57, no. 6, pp. 2171–2179, Jun. 2010.

[14] P. K. Dash, D. P. Swain, A. C. Liew, and S. Rahman, "An adaptive linear combiner for on-line tracking of power system harmonics," *IEEE Trans Power Syst.*, vol. 11, no. 4, pp. 1730–1735, Nov. 1996.

[15] Y. M. Chen and R. M. O'Connell, "Active power line conditioner with a neural network control," *IEEE Trans. Ind. Appl.*, vol. 33, no. 4, pp. 1131–1136, Jul./Aug. 1997.

[16] L. L. Lai, C. T. Tse,W. L. Chan, and A. T. P. So, "Real time frequency and harmonic evaluation using artificial neural network," *IEEE Trans. Power Del.*, vol. 14, no. 1, pp. 52–59, Jan. 1999.

[17] L. H. Tey, P. L. So, and Y. C. Chu, "Improvement of power quality using adaptive shunt filter," *IEEE Trans. Power Del.*, vol. 20, no. 2, pp. 1558–1568, Apr. 2005.

[18] D. O. Abdeslam, P. Wira, J. Merckle, D. Flieller, and Y. A. Chapuis, "A unified artificial neural network architecture for active power filters," *IEEE Trans. Ind. Electron.*, vol. 54, no. 1, pp. 61–76, Feb. 2007.

[19] H. C. Lin, "Intelligent neural network-based fast power system harmonic detection," *IEEE Trans. Ind. Electron.*, vol. 54, no. 1, pp. 43–52, Feb. 2007.

[20] B. Singh, V. Verma, and J. Solanki, "Neural network-based selective compensation of current quality problems in distribution system," *IEEE Trans. Ind. Electron.*, vol. 54, no. 1, pp. 53–60, Feb. 2007.

[21] A. Luo, Z. Shuai, W. Zhu, and Z. J. Shen, "Combined system for harmonic suppression and reactive power compensation," *IEEE Trans. Ind. Electron.*, vol. 56, no. 2, pp. 418–428, Feb. 2009.

[22] G. W. Chang, C. I. Chen, and Q. W. Liang, "A two-stage adaline for harmonics and interharmonics measurement," *IEEE Trans. Ind. Electron.*, vol. 56, no. 6, pp. 2220–2228, Jun. 2009.

[23] J. H. Marks and T. C. Green, "Predictive transient-following control of shunt and series active power filters," *IEEE Trans. Power Electron.*, vol. 17, no. 4, pp. 574–584, Jul. 2002.

[24] M. Routimo, M. Salo, and H. Tuusa, "A novel simple prediction based current reference generation method for an active power filter," in *Proc. IEEE APEC*, 2004, pp. 3215–3220.

[25] B. N. Singh, B. Singh, A. Chandra, and K. Al-Haddad, "Design and digital implementation of active filter with power balance theory," *Proc. Inst. Elect. Eng.—Electr. Power Appl.*, vol. 152, no. 5, pp. 1149–1160, Sep. 2005.

[26] M. H. Rashid, *Recent Development in Power Electronics: Selected Reading*. Piscataway, NJ: IEEE Press, 1996.

[27] S. Kumar, *Neural Networks—A Class Room Approach*. New Delhi, India: Tata McGraw-Hill, 2004.

[28] F. M. Ham and I. Kostanic, *Principles of Neurocomputing for Science &Engineering*. New Delhi, India: Tata McGraw-Hill, 2002.

[29] J. Nocedal and S. J. Wright, *Numerical Optimization*. New York: Springer-Verlag, 1999.

AUTHORS

1. D. GOWTAMI (M.Tech)
   Cell: +9951118245,
   Email: sai.gowtami10@gmail.com
2. S.RAVINDRA M.Tech
   Cell: +9908699825
   Email: s.ravindra.sai@gmail.com
3. A. MALLIKARJUNA PRASAD M.Tech (Ph.d)
   Cell: +9849144565
   Email: mallikarjunaprasad0307@gmail.com
4. G.KISHORE M.Tech (Ph.d)
   Cell: +9618449079
   Email: gudipatikishor@gmail.com

❖ ❖ ❖